Time-dependent Plume Front Positioning and Its Dynamics Coupled With Seasonal River Efflux

G. Seena
CSIR-National Institute of Oceanography, Regional Centre-Kochi
K. R. Muraleedharan (muraleedharan@nio.org)
CSIR-National Institute of Oceanography, Regional Centre-Kochi
C. Revichandran
CSIR-National Institute of Oceanography, Regional Centre-Kochi
S. Abdul Azeez
CSIR-National Institute of Oceanography, Regional Centre-Kochi
Sebin John
CSIR-National Institute of Oceanography, Regional Centre-Kochi
Ravikumar C. Nair
CSIR-National Institute of Oceanography, Regional Centre-Kochi

Research Article

Keywords: Plume Front, Brunt Vaisala Frequency, Richardson Number, Froude Number, South west coast of India

Posted Date: March 11th, 2021

DOI: https://doi.org/10.21203/rs.3.rs-290060/v1

Version of Record: A version of this preprint was published at Ocean Dynamics on February 17th, 2022.
See the published version at https://doi.org/10.1007/s10236-022-01499-8.

Time-dependent plume front positioning and its dynamics coupled with seasonal river efflux

G. Seena[1,2], K. R. Muraleedharan[1*], C. Revichandran[1], S. Abdul Azeez[1], Sebin John[1,2,3] & Ravikumar C. Nair[1]

[1]CSIR-National Institute of Oceanography, Regional Centre-Kochi, Kerala, India.

[2]Research Scholar, Bharathidasan University, Tiruchirapalli, India.

[3]India Meteorological Department, New Delhi.

*email: muraleedharan@nio.org

Abstract

The time-dependent plume front fluctuation concerning different tidal phases and its dynamics coupled with seasonal river efflux in the shelf off Kochi, south west coast of India, were investigated using Finite Volume Community Ocean Model (FVCOM). The region is linked with a monsoonal estuary, featured by mixed semi-diurnal tide (1 m) and exhibited a highly complicated plume pattern. The rivalry between river efflux with tidal phases create plume fronts in the shelf, whose gradients fortified or weakened by mixing dynamics. Eventhough the incessant river efflux in the summer monsoon impart significant momentum in the shelf, the range of frontal fluctuation was curtailed to 2 km by strong monsoon currents. During transient phase of the season (fall inter-monsoon), the tidal forcings on plume positioning overwhelm the shelf currents, such that the plume front fluctuate between 6-17 km (range increased to ~11 km) from the inlet. In low tides, the region near to the inlets was almost homogenized (R_d <1). While, it gets more stratified in high tides due to the transport of high saline ambient water towards the inlet and also by the decreasing kinetic energy (R_d >1). The location of frontal zones suitable for the propagation of nonlinear waves ($F \leq 1$)will change in respect to the competition between river efflux and tide-topography interaction. The strong stratified plume front regions with increased Brunt Vaisala Frequency (BVF) in summer monsoon behave as active zones of non linear wave propagation only when the plume front decelerates from supercritical to subcritical. During dry season, the $F \leq 1$ was satisfied at limited locations, but the absence of BVFmax zone (frequency >0.3 s^{-1}) revealed that the amplitude of such nonlinear waves would be considerably small. The study divulge that tidally pulsating plume front fluctuates between 3-18 km from inlet and also highlights that the propagation of nonlinear waves with considerable amplitude will depend on both the plume front velocity and the Brunt Vaisala Frequency of the water column.

Keywords: Plume Front, Brunt Vaisala Frequency, Richardson Number, Froude Number, South west coast of India.

Introduction

Freshwater/estuarine plumes are one of the momentous sources of nearshore dynamics. The horizontal and vertical extension of such plumes in the shelf creates plume fronts, the locus of which depend on the terrestrial efflux and also to the varying tidal amplitude. The location of the lift off point fluctuates in accordance with the flood and ebb phases of the tidal cycle[1]. The residue of the river/estuarine discharges into the shelf float as a lens over the ambient coastal waters and further transport as buoyancy-driven gravity current. The relaxation of the gravity currents in the shelf region may radiate nonlinear internal waves such that the amplitude of which is comparable with that of waves generated from tide-topography interactions[2]. Previous studies[3] classified plumes in to surface advected, and bottom advected plumes depending on the interaction with bottom topography. These classifications have a strong correlation in determining the locus and offshore spreading of the plume front. The Froude number gives an insight to the flow characteristics of the fronts and also envisages the probability of the nonlinear wave propagation. Plumes are the one that featured by land remnants which are rich in nutrients, suspended sediments, organic and inorganic carbon, etc., eventually affect the biogeochemistry of the coastal ocean[4]. The converging surface fronts[5] in the shelf due to the plumes are often places of high phytoplankton productivity, such that they serve as an important feeding and reproductive habitat for higher trophic organisms[6].

The variability of the plume in the shelf can be identified by tracing the plume/plume front propagation, horizontal/ vertical mixing and its dilution. The study region (shelf off Kochi, southwest coast of India, SWCI) is associated with a monsoonal estuary-Cochin estuary[7], which completely flushes about 42 times in a year[8]. According to Seena et al.,[9], these flushed riverine/estuarine discharges float over the high saline shelf water as a plume. The peculiarity of the buoyant plume in the shelf off Kochi is that it exhibits both the features of small scale and large scale plume, such that during southwest monsoon (SWM) the plume fringe twisted towards the south and in northeast monsoon (NEM) it twisted towards the north in accordance with the seasonal reversing winds and associated coastal currents. To delineate the plume front displacement and its vertical mixing due to tidal interaction, a time series analysis of the plume propagation is needed. This manuscript details the dynamics of freshwater/estuarine plume fronts in the shelf off Kochi by scrupulously analysing the time-dependent interaction of the plume front with the mixed semi-diurnal tide (~1m) and seasonal river efflux.

Methods

The shelf off Kochi (Fig. 1) is associated with the largest estuary in the west coast of India is always refreshed by a surfeit of annual river discharge (22x10 ^{6} m^3) from hinterland rivers. The region is influenced by the summer monsoon (SM), fall inter-monsoon (FIM), winter monsoon (WM) and spring inter-monsoon (SIM) with varying monthly average river discharge of 1749 m^3/s, 1312 m^3/s, 219 m^3/s, 121 m^3/s in July, October, December and March respectively (Central water commission data (CWC), 2014). The interaction of the plume with the tide and topography along the SWCI was articulated by the Finite Volume Community Ocean Model (FVCOM, v.4.1) for the year 2014. FVCOM is an unstructured grid, finite-volume, free surface, three-dimensional primitive equation coastal ocean model that solves the momentum, continuity, temperature, salinity and density equations[10]. The spatial resolution of the model was assorted from 20 m within 10 km area of the inlet to 50 km towards the open ocean and featured by 60,000 elements with 21 vertical sigma levels. Global self-consistent, hierarchical high-resolution geography database available at http://www.soest.hawaii.edu/wessel/gshhg/ was utilised for delineating land-water interface, while estuaries and backwaters were incorporated by digitising LISS-III data. European Center for Medium Weather Forecast (ECMWF) data was used for surface meteorological forcings, while tidal elevation data was generated from FES 2014 and forced from the open boundary. The river discharge data from CWC was taken as the stimuli for freshwater in the river boundary for the year 2014. The inputs (temperature, salinity and currents) of open boundary were forced from global Hycom model (http://tds.hycom.org/thredds/catalog.html). The utmost timestep for the model was 1s, and the outputs were recorded at every hour. The calibrations and validations of the model were detailed in the paper published by Seena et al.,[9]. Validated model results (24-hour data collected on 15th day of every month) have been used for studying the plume front dynamics, its fluctuation with respect to tides and coastal processes off Kochi.

Computation

In stratified water column (plume influenced regions), quantification of stability parameter gives an insight to the convection processes. Hesselberg defined the stability of the water column as

$$E = -\frac{1}{\rho}\{\frac{\partial \rho}{\partial S}\frac{\partial S}{\partial z} + \frac{\partial \rho}{\partial T}\left(\frac{\partial T}{\partial z} + \Gamma\right)\}m^{-1}$$

where ρ, S, T is the density, salinity and temperature of the water parcel (plume), z is the depth and T is the adiabatic temperature gradient. On approximation, E can be written as

$$E = -\frac{1}{\rho}\frac{\partial \rho}{\partial z}$$

The "Brunt Vaisala Frequency (N)" in a stratified medium is given by,

$$N = \sqrt{gE}\ rad\ s^{-1}$$

Bulk Richardson number is the ratio of the potential energy (PE) to the kinetic energy (KE) and is a useful tool for parameterising the mixing process and can be written as

$$R_d = \frac{\Delta\rho g d}{\rho u^2}$$

where $\Delta\rho$ is the difference in density between the adjacent layer, d is the depth of the water column, ρ the density and u the mean velocity of each layer.

To study the possibility of the free wave propagation in the plume fronts, the Froude number[11] has been calculated as

$$F = \frac{U}{C}$$

U is the plume front velocity, and C is the internal wave speed in the medium in which the wave advances. When $F \leq 1$,supercritical flow becomes subcritical and sets the criterion for free wave propagation [2].

Results

The study region experiences four seasons with considerable variation in the river efflux. The quantity of freshwater efflux peaked in the SM and dropped to a minimum in the SIM. The study by Seena et al.,[9] revealed that the plume behaviour would vary from freshwater plume to estuarine plume in respect to the seasonal river discharge thereby gradients in the frontal zones fortifies or weakens in respect to the season.

The plume front positioning with respect to the tides (Fig. 2) reckons the distance travelled by the front in each tidal phase. In the SM, during LLT (Lowest Low Tide) the front (18 psu contour) occurred at a distance of ~10 km from the inlet, which further extended up to 12 km in HHT (Highest High Tide), again decreased to 10 km in HLT (Highest Low Tide) then increased to 12 km in LHT (Lowest High Tide). The signature of frontal zone (30 psu contour) in the FIM was noted at <6 km at HLT and extended to 12 km in LHT. During LLT the front was discernible at 15 km from the inlet, and in LHT it prolonged to 17 km. In the WM, the freshwater efflux was reduced, and the front was identified by the 34 psu contour whose offshore extension corresponding to HHT, LLT, LHT, and HLT was 12 km, 9 km, 14 km and 13 km respectively. SIM is the dry season of the region with comparatively declined river efflux where the front (34 psu contour) extended up to 8 km in LHT and confined to 4 km in HLT.

During the SM, the river efflux of about 1749 m^3/s reached the shelf and formed the freshwater plume over the ambient shelf water. In LLT the front touched the bottom up to a distance of 1 km from the inlet, after that the frontal zone got detached from the bottom and extended towards offshore up to 10 km (Fig. 3). The BVF maximum (BVFmax) zone with frequency >0.3 s^{-1} was observed between 5-10 km from the inlet in respect to the stability of the water column. During this period, R_d is <1 near to inlets and >1 towards offshore. Also, the variation in front velocity with wave velocity was well depicted in the F values. During the HHT the plume float as a thin lens over the shelf water having thickness ~1 m while the offshore extension was found to be more than the LLT. In respect to the plume spreading the pattern of BVF changed such a way that the BVFmax zone extended horizontally (~ 9 km) along the surface. R_d was >1 throughout the plume spread region, and the probability for nonlinear wave propagation was higher. After 6 hours from HHT, the plume was influenced by HLT (Supplementary Fig. 1) where the front touched the bottom up to a distance of 0.5 km, further detached from the bottom and extended towards offshore ~10 km from the inlet. The BVFmax zone lies near to surface, but the spreading of it was limited to <5 km from the inlet. The strong outward flow (maximum KE) observed in the inlet region overcomes the buoyancy (PE), which was well depicted in the R_d values. Away from the inlets, the flow velocity decreased abruptly and eventually resulted in an area having R_d > 1. The F<1 condition was limited only to a small area in the front. Due to the effect of LHT, the front further detached from the bottom and resulted in the increased offshore extension as a thin layer over the shelf (~11 km) water. The pattern of BVFmax, R_d and F were changed in respect to the front spreading, which was much similar to that in the HHT.

The FIM was featured by a decreased monthly average river discharge of about 1312 m^3/s; accordingly, we considered the 30 psu contour (estuarine plume) to isolate the plume front. In the HLT (Supplementary Fig. 2), even though the outward tidal flow was active, the front did not touch the bottom, and it spread only up to a distance of 5 km from the inlet. The BVFmax lies only within a small area where the R_d was >1. The F values revealed that the chances of nonlinear wave propagation were limited under this condition. After 6 hours, the plume was modulated by LHT such a way that the thickness of the plume remains same as HLT, but the offshore extension increased up to 13 km. The pattern for BVFmax and RN were changed according to the plume spreading, while the lower values of F (<1) implied the possibility of wave generation in the frontal zones. Further, the plume was affected by LLT (Fig. 4) where the front touched the bottom for a few kilometres (<1 km) and detached subsequently. Due to

the strong pulling in the LLT, the plume offshore extension was increased to 15 km. The spreading of BVFmax zone was increased throughout the front zone where R_d was always >1, but the possibility for free wave propagation was limited to the inlets only. The influence of the HHT on the plume make it as a very thin lens over the ambient shelf water with an offshore extension of 17 km and uniform thickness of <1m. The BVFmax zone maintained a similar spatial extension as that of the plume with R_d>1. A smaller value of F <1 noticed near to the inlets in the surface layers with a limited area of spreading.

WM is the 3rd phase of the seasonal change associated with the shelf where the river efflux was ceased to 219 m^3/s. The shelf was lacked by freshwater efflux such that we consider the 34 psu contour for identifying the estuarine plume influenced area or demarcating the plume front. During the HHT (Fig. 5), the front was identified as a thin layer over the ambient shelf water with an extension of 12 km from the inlet. The BVFmax zone cannot be defined under this condition where the maximum frequency was about 0.2 s^{-1}. Buoyancy energy and the R_d exhibited a similar pattern to that of the plume, but the F <1 condition was satisfied in restricted regions of the front. During the LLT, the plume touched the bottom up to a distance of 1 km from the inlet; afterwards, it detached and extended up to 9 km towards offshore direction. The BVFmax zone was very thin, and R_d was varied as per the energy of the plume, while F<1 condition existed below the considered frontal zone. Further, the plume was acted upon by LHT (Supplementary Fig. 3) such that the front detached from the bottom and extended horizontally to 14 km. The BVFmax zone was noticed as a thin film in the shelf region, but due to the reduced flow velocity, R_d>1 condition was satisfied by a broad area in the plume influenced zone. The probability of nonlinear wave propagation was more within a distance of 5 km from the inlet. After 6 hours, the plume was modified by HLT such a way that both the horizontal extension of the plume (13 km) and the BVFmax zone were reduced. The pattern of R_d and F were similar to that in the LHT condition.

SIM is the dry phase among the season, where the monthly average river efflux into the estuary was reduced to 121 m^3/s. The salinity changes due to the river effluxes were scanty, and hence the 34 psu contour was used to delineate the plume front. During the LLT (Fig. 6), the front neither touched the bottom nor extended beyond 6 km. The region within the front was lack of BVFmax zone where the maximum possible frequency was up to 0.1s^{-1}. Due to the reduction in PE, the area having R_d>1 was negligibly small in the shelf region. The F values divulged that the chances of wave propagation were not satisfied in the LLT phase. Further, the plume was amended by LHT (Supplementary Fig. 4) such that the flood tide modified the plume

198 pattern into a thin layer over the inshore water. Due to the upward pushing of tides, the offshore
199 spreading of the plume was increased to 8 km. The BVF was increased to 0.25 s^{-1}, and the
200 spatial area of the plume having R_d>1 was extended. During the HLT, the plume extension
201 was reduced to <5 km, concurrently the BVF and R_d were also modified. Due to the negligible
202 density gradients in the water column, the possibility of nonlinear wave propagation in the
203 frontal region was insignificant. After 6 hours, the plume was influenced by the HHT (Fig. 6)
204 by which its thickness reduced to 1 m from 7 m (HLT) near to the inlet, and the offshore
205 spreading increased to 7 km from 4 km. Even though the frontal zone satisfied the condition
206 of nonlinear wave propagation, the frequency of oscillation of water column was greatly
207 reduced.
208
209 **Discussion**
210 Plume front is the narrow region in the shelf where the physical properties changes abruptly;
211 forming a boundary between the outward flowing buoyant water over the ambient coastal
212 water[5]. As fronts serve as the biological hotspots, it is imperative to understand the offshore
213 limit of plume fronts due to tide-topography interaction. In this paper, we analysed the
214 fluctuation of plume front positioning in respect to the tides and details about buoyant plume
215 stability, BVF, condition for nonlinear wave propagation etc.,
216 The SM is featured by incessant river discharge that overwhelmed the tidal forcing to maintain
217 the frontal position (Fig. 2) between 10 km (low tide) - 12 km (high tide). The expected offshore
218 extension of the front due to tides and turbulent KE was not evident, which was curtailed by
219 the strong SWM currents. Even though the data was taken in the spring tide, the heavy river
220 efflux act as a barrier to the intrusion of high saline water into the estuary by tidal currents.
221 During the low tide, enhanced efflux from the estuary strengthened the front to touch the
222 bottom (lift off point is about 1 km from the inlet), while the consecutive high tide uplifted the
223 front from the bottom and elongated towards offshore (Fig. 3 and Supplementary Fig. 1). The
224 time-series data revealed that the flood currents were not adequate to increase the salinity of
225 the estuary > 18 psu due to the heavy river efflux. The protrusion of these modified low saline
226 water (18 psu) over the ambient water serves as an “estuary at sea” in the monsoon season. The
227 BVFmax zone always lies away from the inlet due to the fact that the vertical gradients were
228 maximum at a certain distance from the inlet. In low tide, the water column near to the inlets
229 was homogenised (mixing) due to increased KE (R_d<1). After travelling a few distances from
230 the inlet, the plume velocity decreased such that the KE is not adequate to homogenise the

water column (R_d>1). During the high tide, high saline water, flow towards the inlet and the plume extended as a lens over the shelf water. The water column was more stratified under this condition with greater PE, which was well reflected in the high R_d values. The F≤ 1 was satisfied in the near-surface waters of the frontal zone (within 1 m towards offshore and 7.7 m in inlets), while the BVFmax zone always lies <2.5 m during all the tidal phases.

The freshwater efflux into the estuary was declined in the FIM season, and the shelf region experienced a transition from SWM to NEM. The positioning of the front was well coupled with varying tidal phases, and river efflux (Fig. 2) where the maximum frontal extension was ~17 km during the HHT and minimum was ~5 km in HLT. Due to the weakening of coastal currents in the FIM, the tidal currents and plume momentum played a significant role in frontal positioning, such that the range of frontal fluctuation was about 12 km, which was much more than the SM (2 km). Except for the LLT, the plume floated as a lens over the shelf water throughout all the tidal phases (Supplementary Fig. 2 and Fig. 4). The BVFmax was always lying near to the surface, and maximum spreading during the HHT was driven by the upward pushing of high saline water. Even though the extension of BVFmax zone was higher, the condition for nonlinear propagation of waves was satisfied within a limited zone (<5 km). This is because of the fact that within this 5 km, the front velocity decelerates such a way that the plume flow changes from supercritical to subcritical and the rate of conversion of KE into PE was increased (R_d>1).

In the WM, the shelf region was controlled by the northward-flowing currents and hence the plume fringe twisted towards the north[9]. The competition between river efflux and shelf dynamics defined the degree of stratification in the water column. The range of frontal fluctuation was about 6 km (Fig 2), which was lesser than the FIM and was mainly due to the declined river efflux. Even though the horizontal and vertical extension was maximum in the LHT (Fig. 5), the BVFmax zone was vivid as a thin layer close to the surface. Throughout all the tidal phases (Fig. 5 and Supplementary Fig. 3), the condition F≤ 1 was satisfied up to a distance of <5 km from the inlet, but the amplitude of such waves may be feeble due to the reduced stratification.

The river efflux was significantly reduced in the SIM such that the KE in the shelf zone due to plume was negligibly small compared to that of tidal flow. The effect of tidal forcings on these limited buoyancy inputs (Fig. 6 and Supplementary Fig. 4) was more than the shelf dynamics/currents due to the tranquil nature of the season. The BVF was varied with respect to the plume positioning. At the same time, the absence of BVFmax zone revealed that the

perturbance in the water column would generate only oscillations with a lesser amplitude that cannot be compared with that in the monsoon season.

Conclusion

The manuscript detailed the dynamics of the time-dependent buoyant outflow with respect to the different tidal phases in the shelf off Kochi, SWCI. The interaction of the seasonal river efflux with the mixed semi-diurnal tide create plume fronts (frontogenesis) in the shelf whose gradients fortified or weakened by the mixing dynamics. After protruding out of the vent (Fort Kochi inlet), the plume float over the shelf water throughout all the tidal phase except at low tides in which the plume touched the bottom up to a certain distance (<1 km) from the inlet, thereby exhibit the features of the surface advected plume. In the SM, the offshore extension of the plume front was initially driven by the quantity and momentum of freshwater efflux, and the tidal currents, which was curtailed (range of fluctuation was <2km) by the strong SWM currents prevailed during this season. In contrast, in the transient phase (FIM) of the season, the tidal forcings and the plume energy overwhelmed the shelf dynamics/currents and played a significant role in frontal positioning (range of frontal fluctuation was about 11 km). In the low tides, the region near to the inlets were almost homogenised (R_d<1), whereas it gets more stratified in the high tides due to the transport of high saline ambient water towards the inlet and also by the decreasing KE (R_d>1). Even though strong stratification in the shelf waters was induced by the heavy river efflux, the condition of the propagation of nonlinear waves was satisfied only when the front velocity decelerates from supercritical to subcritical. Thus, the location of frontal zones suitable for the nonlinear wave propagation will change in respect to the competition between river efflux and tide-topography interaction. During the lean discharge period, the condition $F \leq 1$ was satisfied at limited locations, but the absence of BVFmax zone revealed that the amplitude of such nonlinear waves would be considerably small. The study divulged that the tidally pulsating plume front fluctuate between 3 km from inlet to ~18 km towards offshore due to the shelf dynamics and also highlights that the propagation of nonlinear waves with considerable amplitude will depend on both the front velocity and the BVF of the water column.

Data Availability Statement

The data utilized for land water-interface and bathymetry (GEBCO) were available online at http://www.soest.hawaii.edu/wessel/gshhg/ and at (https://download.gebco.net/) respectively.

Model forcings can be obtained from ECMWF (https://apps.ecmwf.int/datasets/data/interim-full-daily/levtype=sfc/). The open boundary inputs were accessible from global Hycom model (http://tds.hycom.org/thredds/catalog.html). Model data will be available upon request to the corresponding author and the in-situ data used for model validation will be available upon request to CSIR-NIO data repository (www.nio.org).

References

1. Jay, D. A. & Smith, J. D. Residual circulation in shallow estuaries: 1. Highly stratified, narrow estuaries. *J. Geophys. Res. Ocean.* **95**, 711–731 (1990).
2. Nash, J. & Moum, J. N. River plumes as a source of large-amplitude internal waves in the coastal ocean. *Nature* **437**, 400–403 (2005).
3. Yankovsky, A. E. & Chapman, D. C. A simple theory for the fate of buoyant coastal discharges. *Oceanogr. Lit. Rev.* **3**, 435 (1998).
4. J. Dagg, M., Benner, R., Lohrenz, S. & Lawrence, D. Transformation of dissolved and particulate materials on continental shelves influenced by large rivers: Plume processes. *Cont. Shelf Res.* **24**, 833–858 (2004).
5. Garvine, R. W. & Monk, J. D. Frontal structure of a river plume. *J. Geophys. Res.* **79**, 2251–2259 (1974).
6. Morgan, C. A., De Robertis, A. & Zabel, R. W. Columbia River plume fronts. I. Hydrography, zooplankton distribution, and community composition. *Mar. Ecol. Prog. Ser.* **299**, 19–31 (2005).
7. Vijith, V., Sundar, D. & Shetye, S. R. Time-dependence of salinity in monsoonal estuaries. *Estuar. Coast. Shelf Sci.* **85**, 601–608 (2009).
8. Revichandran, C. *et al.* Environmental set-up and tidal propagation in a tropical estuary with dual connection to the sea (SW Coast of India). *Environ. Earth Sci. - Env. EARTH SCI* **66**, (2012).
9. Seena, G., Muraleedharan, K. R., Revichandran, C., Azeez, S. A. & John, S. Seasonal spreading and transport of buoyant plumes in the shelf off Kochi, South west coast of India-A modeling approach. *Sci. Rep.* **9**, 1–15 (2019).
10. Chen, C., Liu, H. & Beardsley, R. C. An unstructured grid, finite-volume, three-dimensional, primitive equations ocean model: application to coastal ocean and estuaries. *J. Atmos. Ocean. Technol.* **20**, 159–186 (2003).
11. Kilcher, L. F. & Nash, J. D. Structure and dynamics of the Columbia River tidal plume front. *J. Geophys. Res. Ocean.* **115**, (2010).

Acknowledgements

The study was funded by Department of Science and Technology under WOS-A scheme (GAP 2908), and the author is very thankful to DST. The authors are grateful to the Director, CSIR-NIO and SIC, NIO-RC Kochi for giving an opportunity for fulfilling the studies. A special acknowledgement for FVCOM development team members in The Marine Ecosystem Dynamics and Modeling Laboratory, UMASSD for providing FVCOM source code.

Author Contributions

Seena, G., (G.S.), Muraleedharan, K.R., (K.R.M.), Revichandran, C., (C.R.), Abdul Azeez, S., (S.A.A.), Sebin John, (J.S.) and Ravikumar C. Nair, (R.C.N.); G.S. managed the funding, data analysis and writing of the manuscript; K.R.M. conceived the problem, field survey, analysis and interpretation of the data; C.R. oversaw the project, involved in the discussion and draft preparation; K.R.M., S.A.A., G.S., J.S., and R.C.N., involved in the modelling studies; G.S., S.A.A., and R.C.N., prepared the figures and model validation diagrams. All authors reviewed the manuscript.

Competing Interests

The author(s) declare no competing interests.

Additional information

Correspondence and requests for materials should be addressed to K.R.M.

365 **Figures**

366

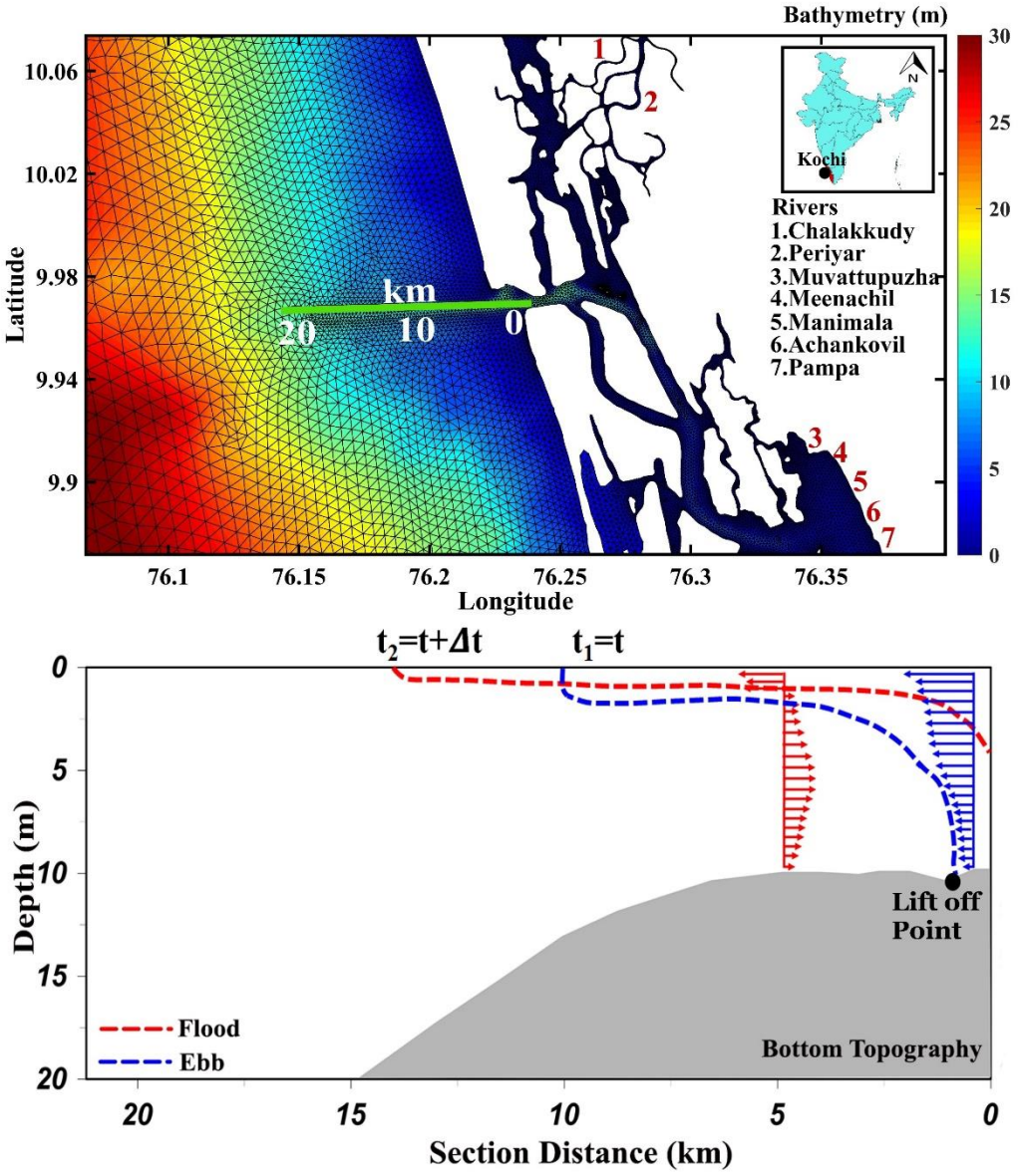

367

368 Figure 1. The geographical area (upper panel) of SWCI articulating finite elemental grid for
369 the FVCOM study. The interaction of front during flood and ebb phase of tide with bottom
370 topography was detailed in the lower panel.

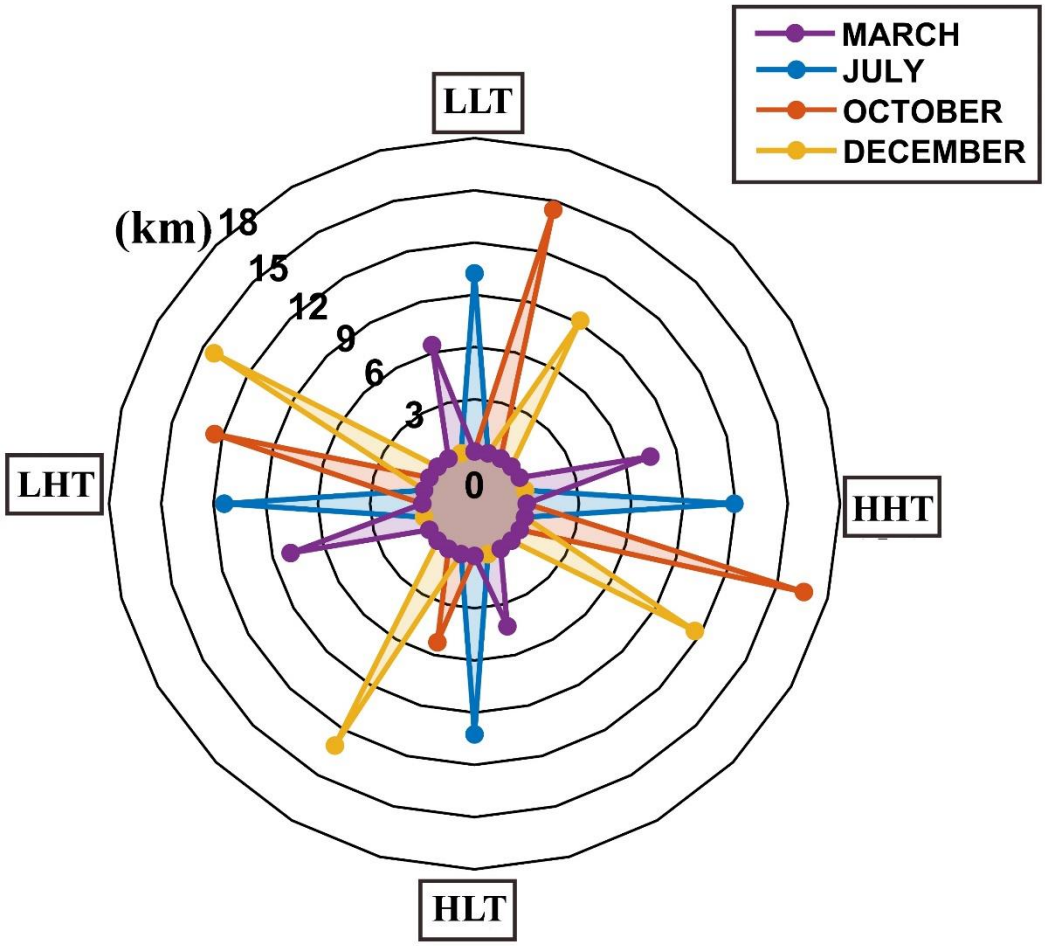

371

372 Figure 2. Divulge the time-dependent plume front positioning in respect to varying tidal phases
373 and seasonal river efflux.

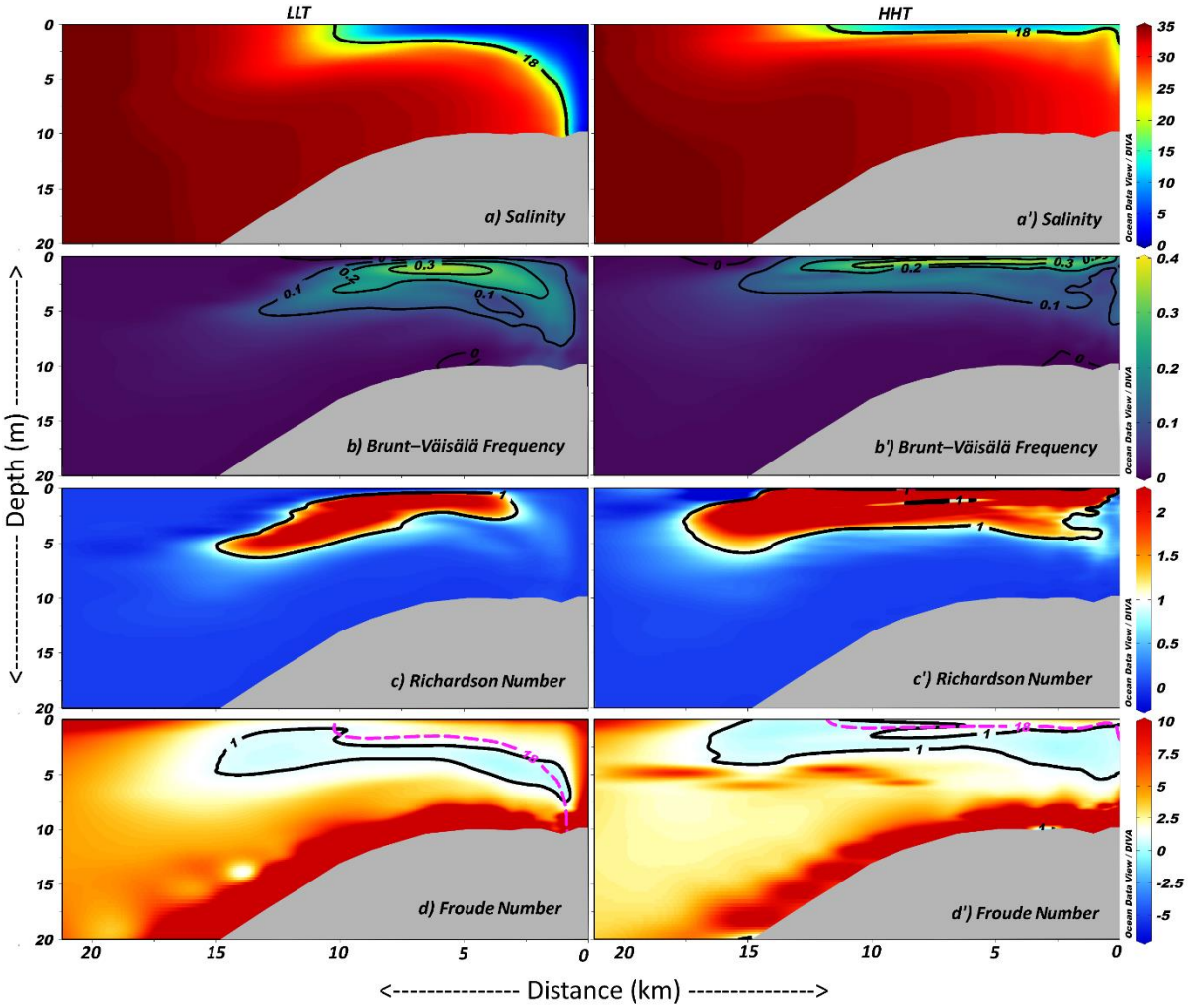

Figure 3. The horizontal and vertical extension of front, and variations in BVF,R_d, and F in the SM during LLT and HHT.

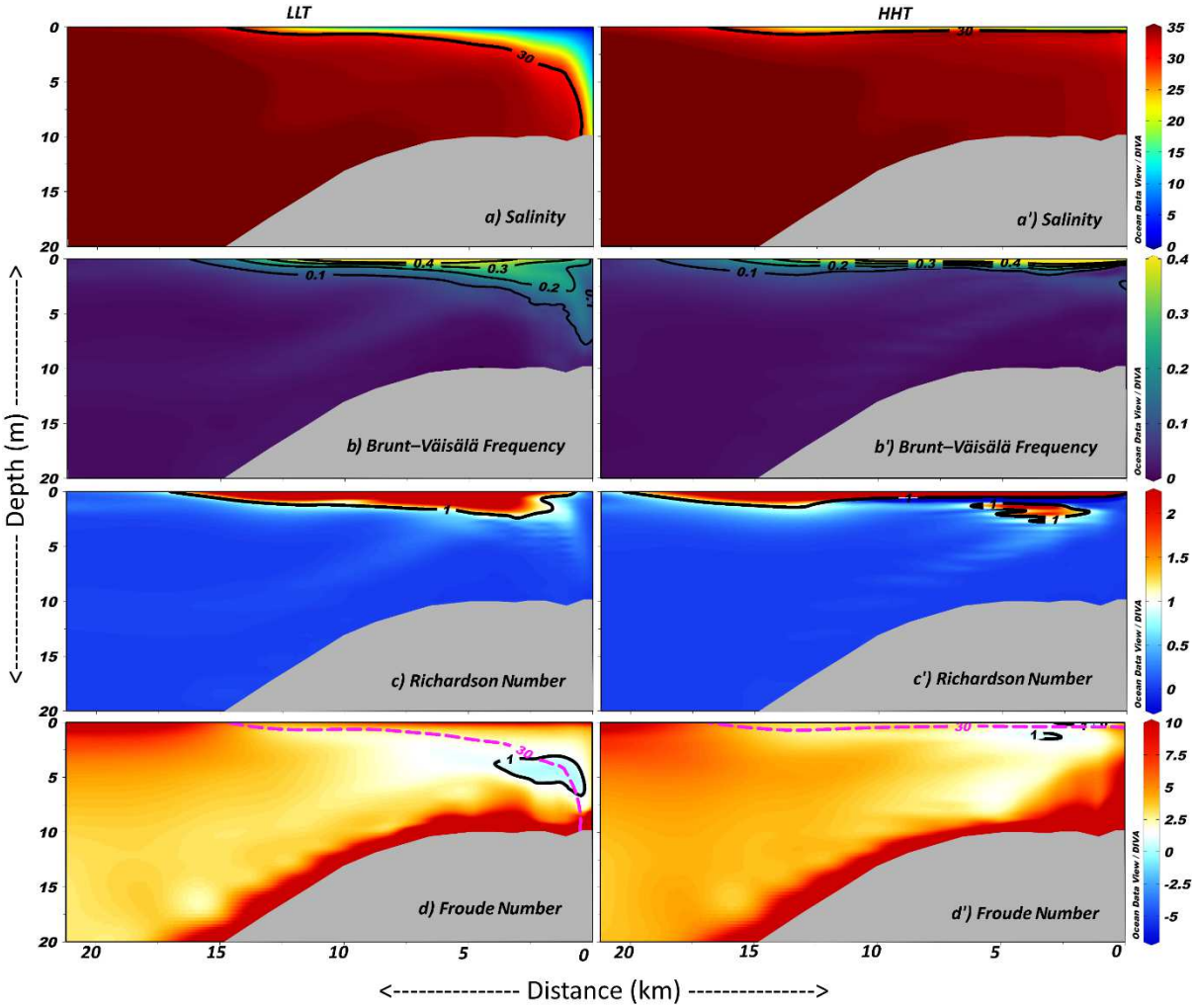

377

378 Figure 4. The horizontal and vertical extension of front, and variations in BVF,R_d, and F in the

379 FIM during LLT and HHT.

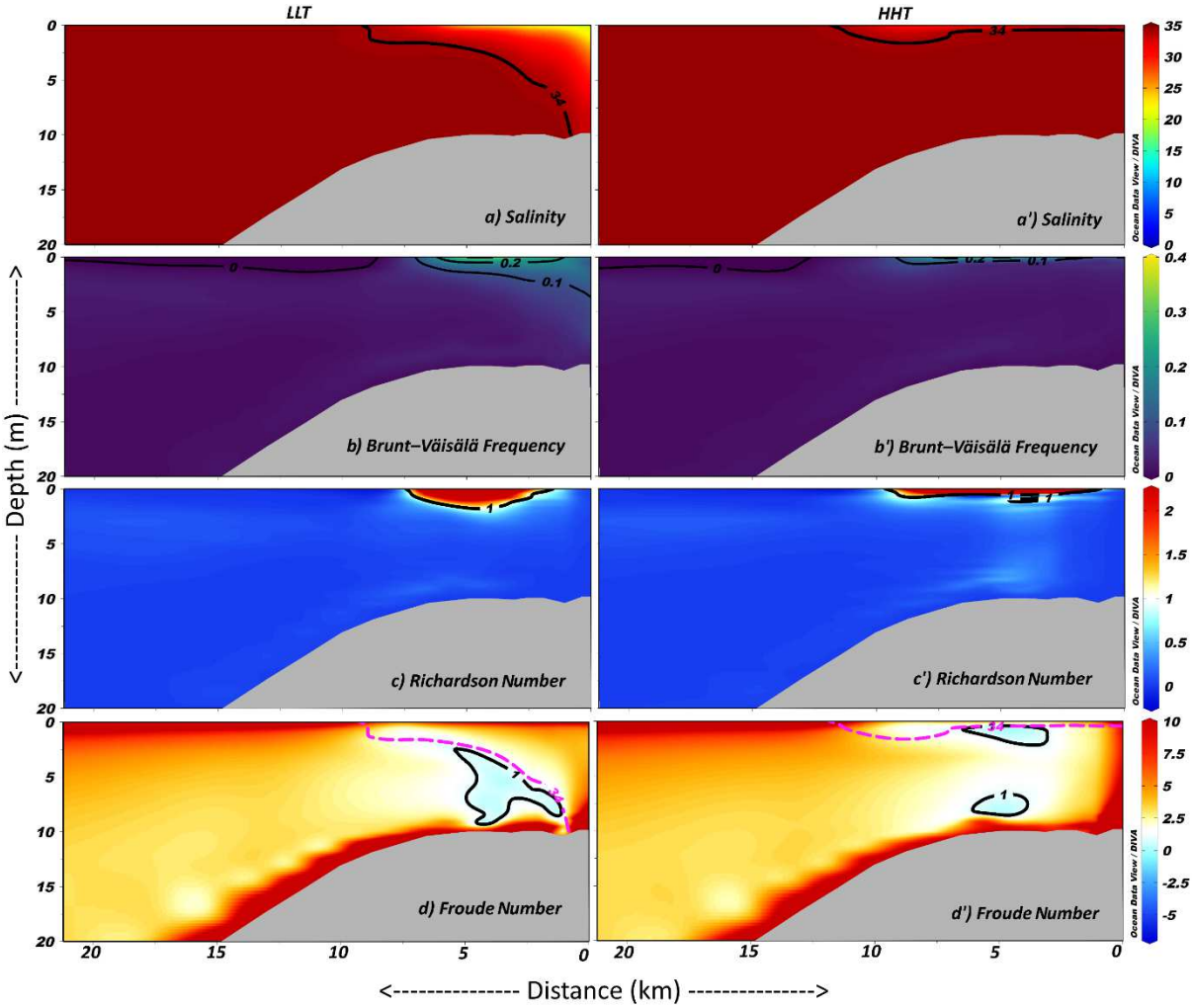

Figure 5. The horizontal and vertical extension of front, and variations in BVF,R_d, and F in the WM during LLT and HHT.

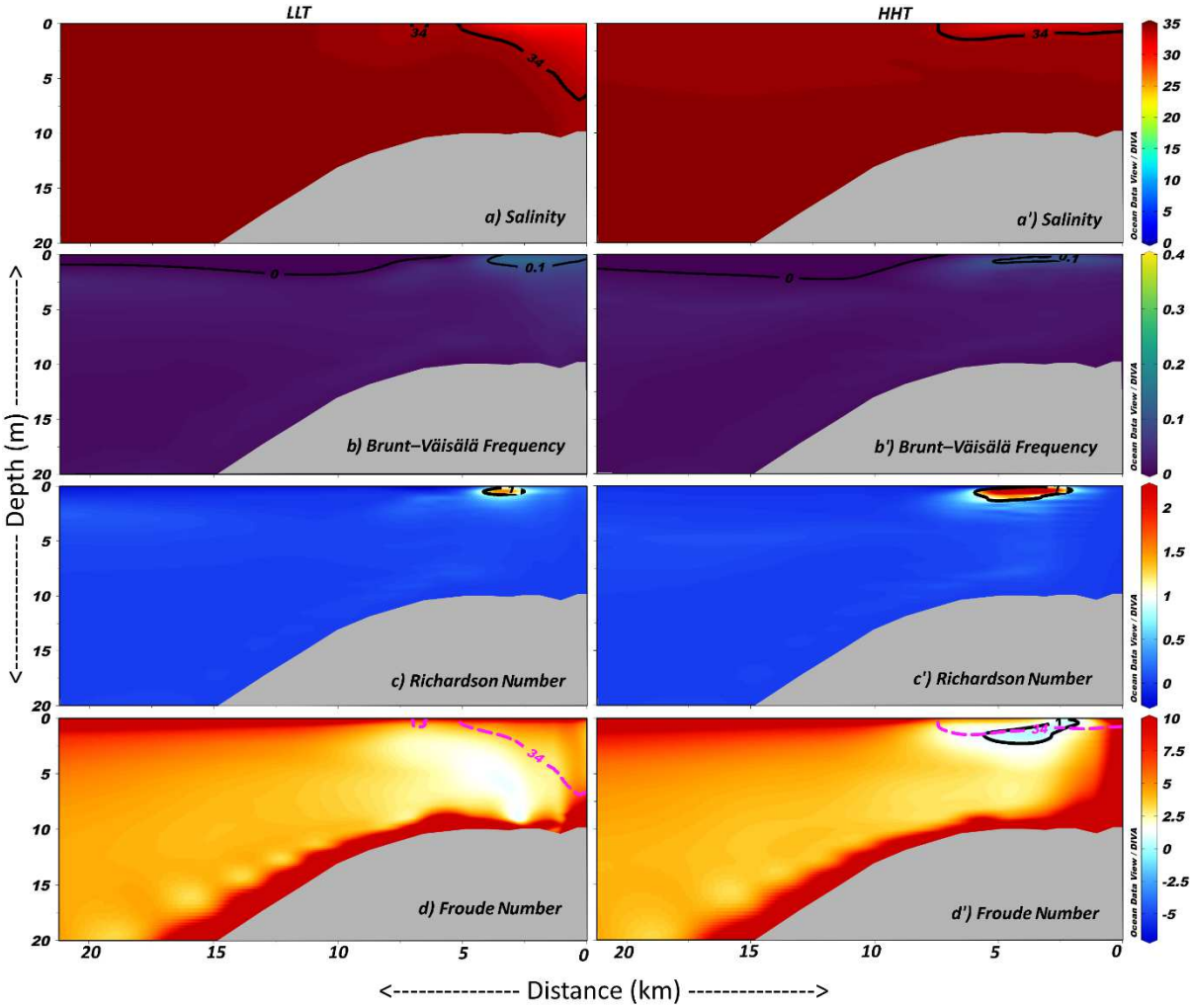

Figure 6. The horizontal and vertical extension of front, and variations in BVF,R_d, and F in the SIM during LLT and HHT.

Figures

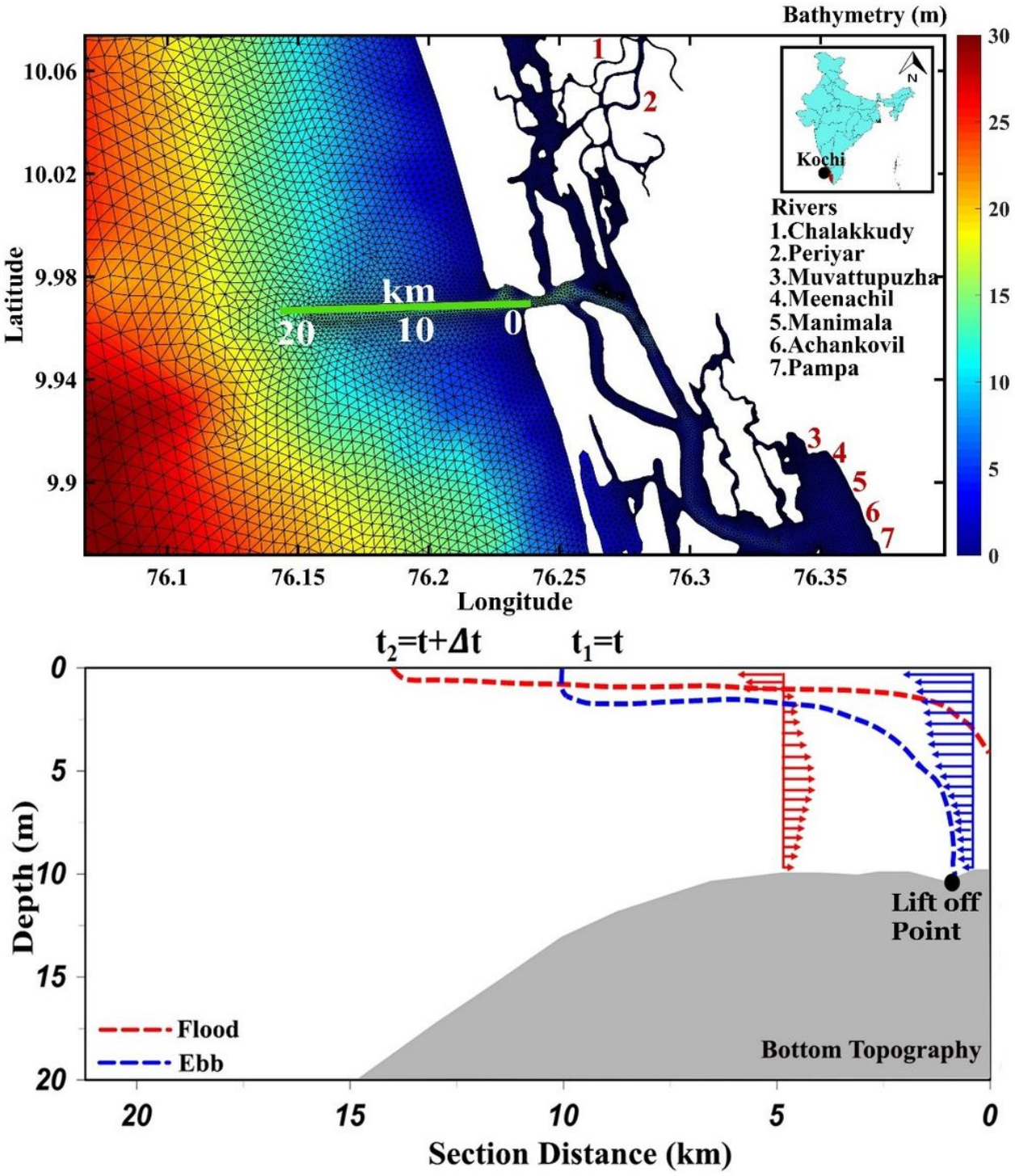

Figure 1

The geographical area (upper panel) of SWCI articulating finite elemental grid for the FVCOM study. The interaction of front during flood and ebb phase of tide with bottom topography was detailed in the lower panel. Note: The designations employed and the presentation of the material on this map do not imply the expression of any opinion whatsoever on the part of Research Square concerning the legal status of

any country, territory, city or area or of its authorities, or concerning the delimitation of its frontiers or boundaries. This map has been provided by the authors.

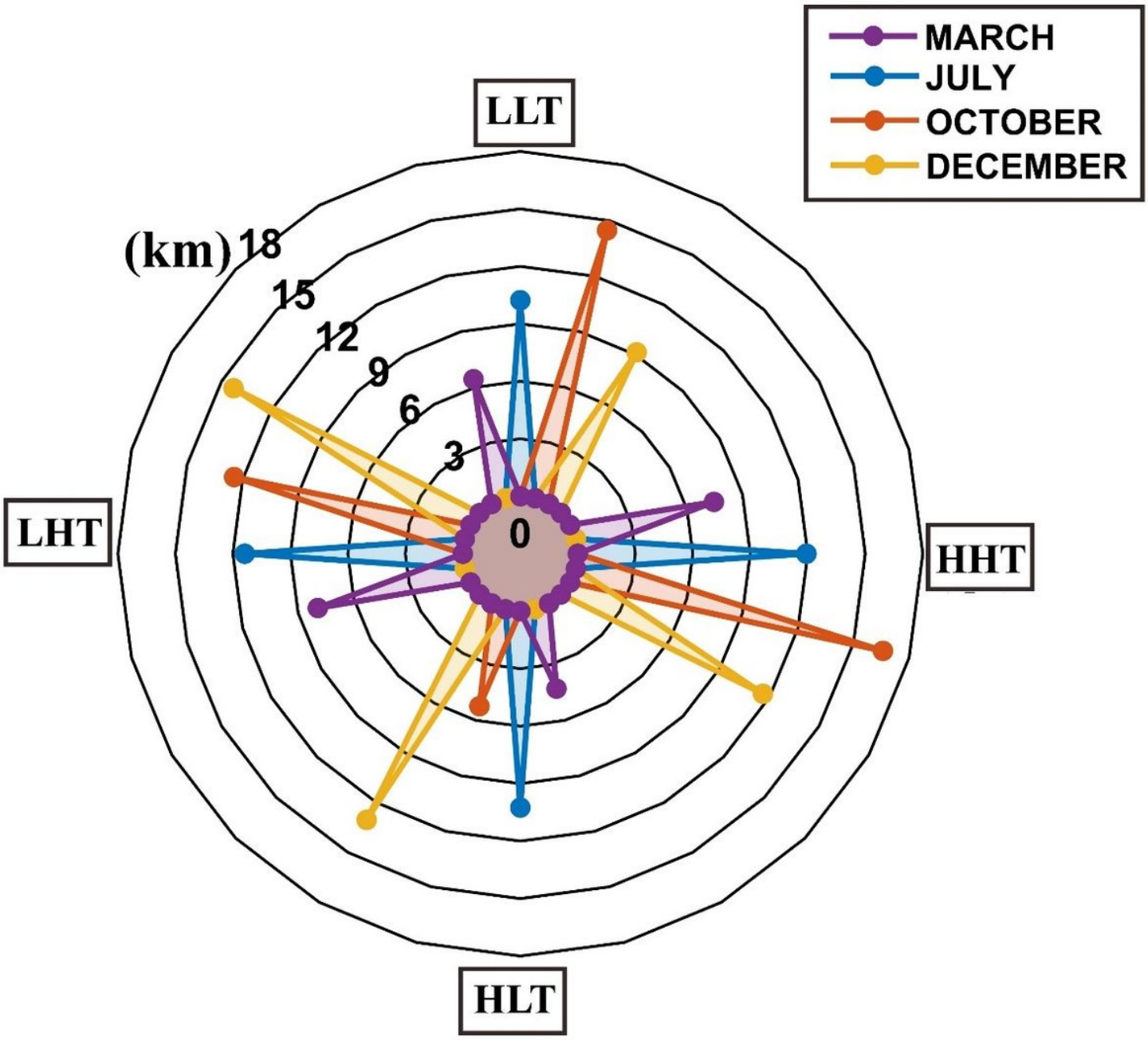

Figure 2

Divulge the time-dependent plume front positioning in respect to varying tidal phases and seasonal river efflux.

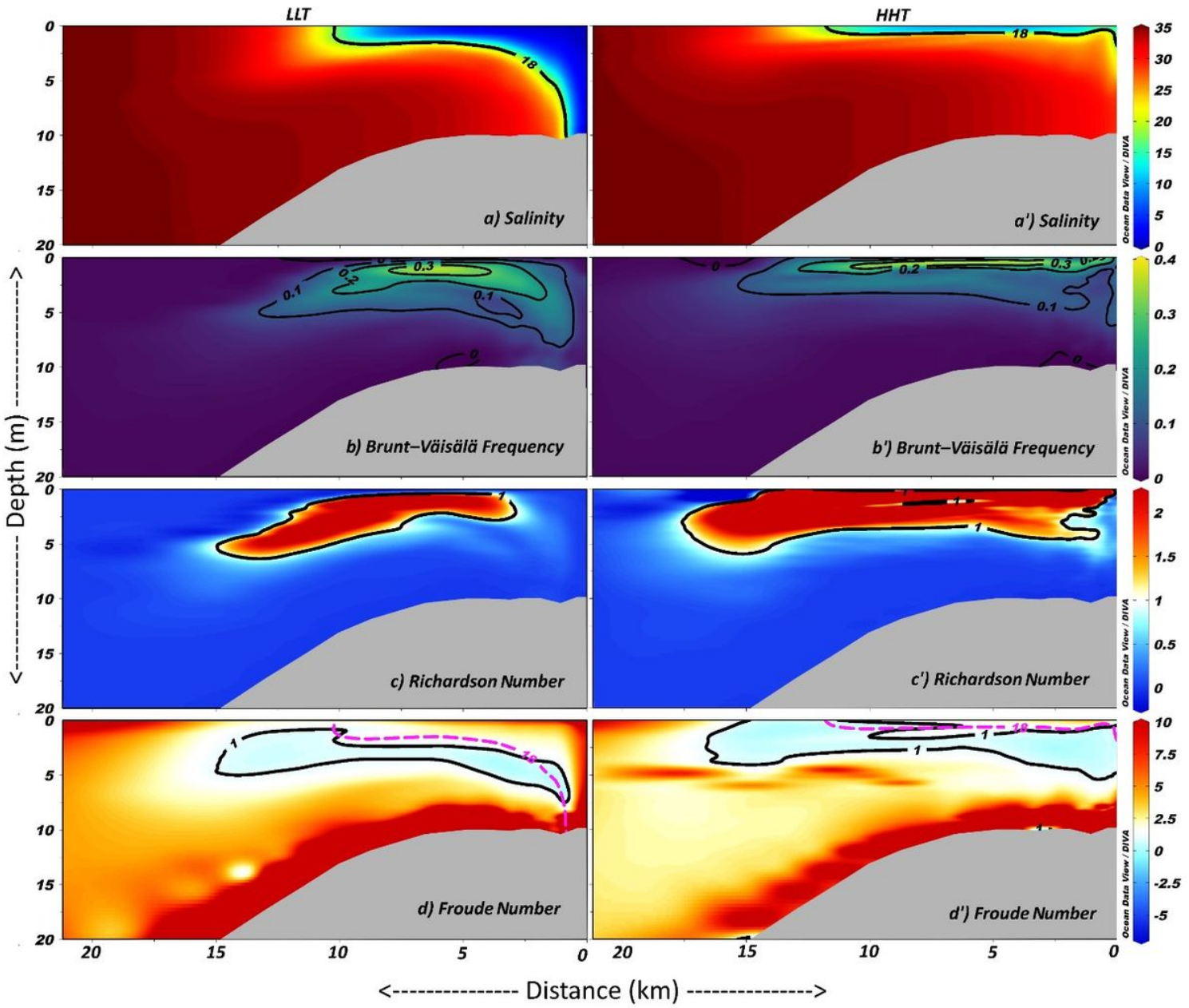

Figure 3

The horizontal and vertical extension of front, and variations in BVF, Rd, and F in the SM during LLT and HHT.

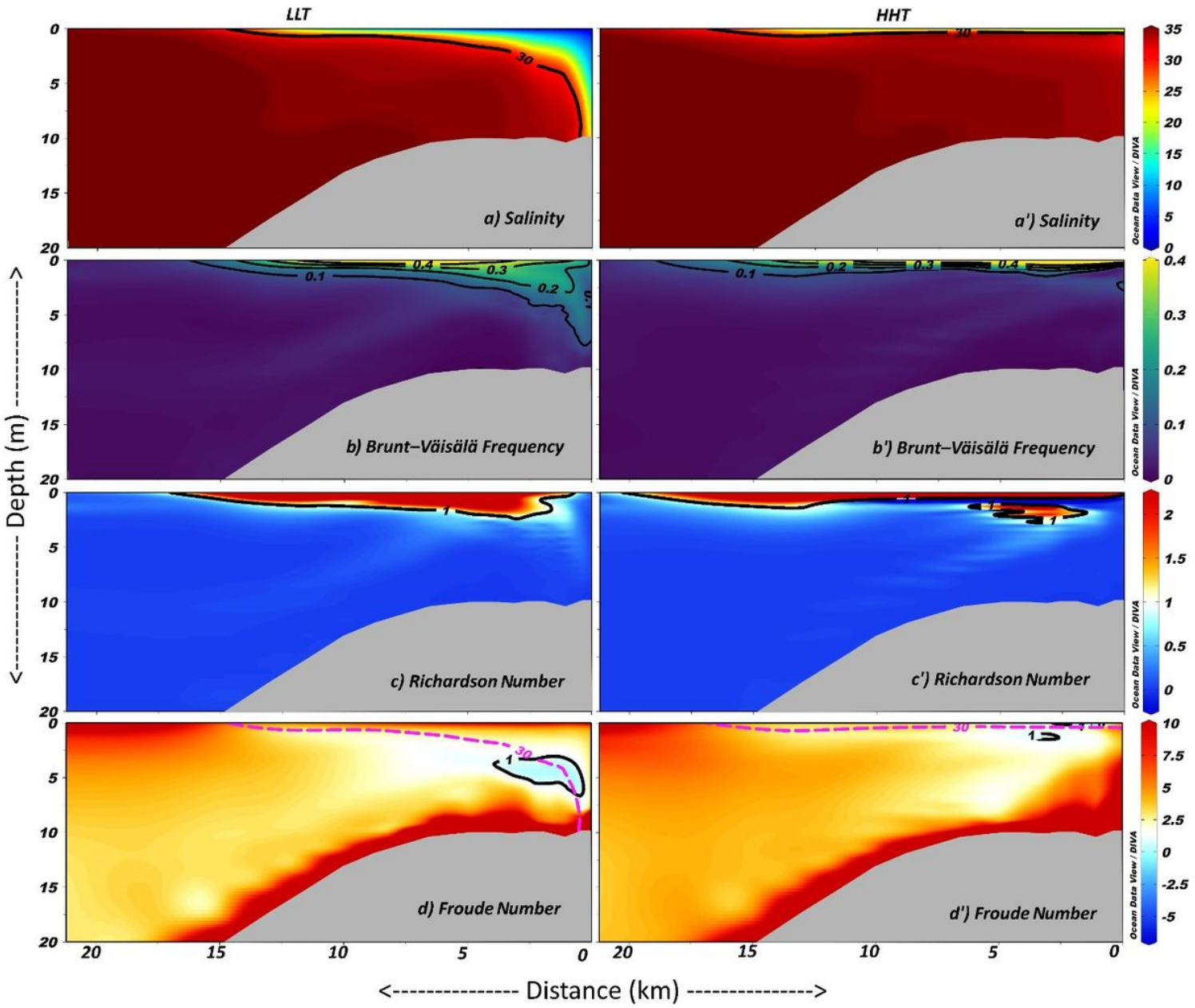

Figure 4

The horizontal and vertical extension of front, and variations in BVF, Rd, and F in the FIM during LLT and HHT.

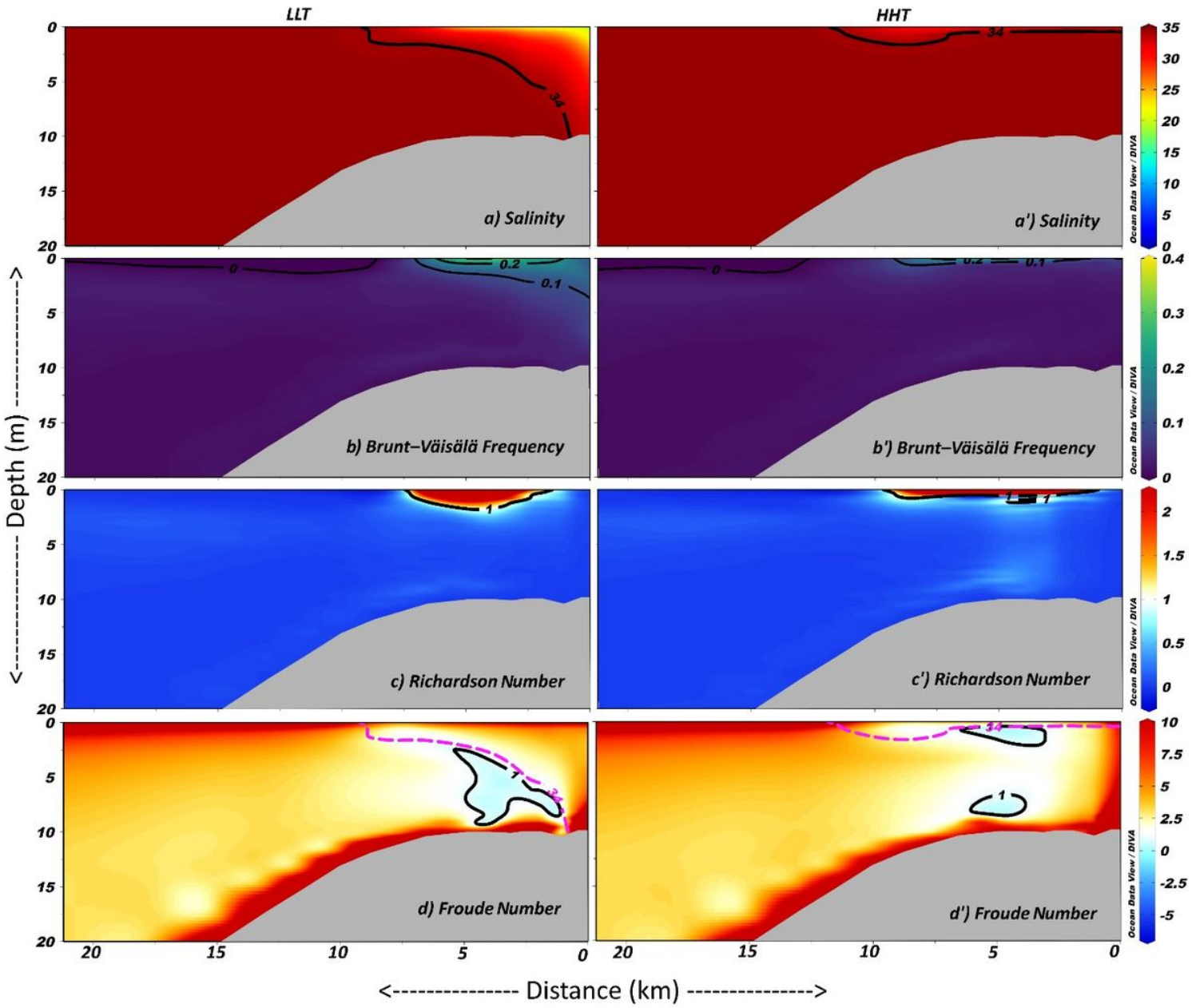

Figure 5

The horizontal and vertical extension of front, and variations in BVF, Rd, and F in the WM during LLT and HHT.

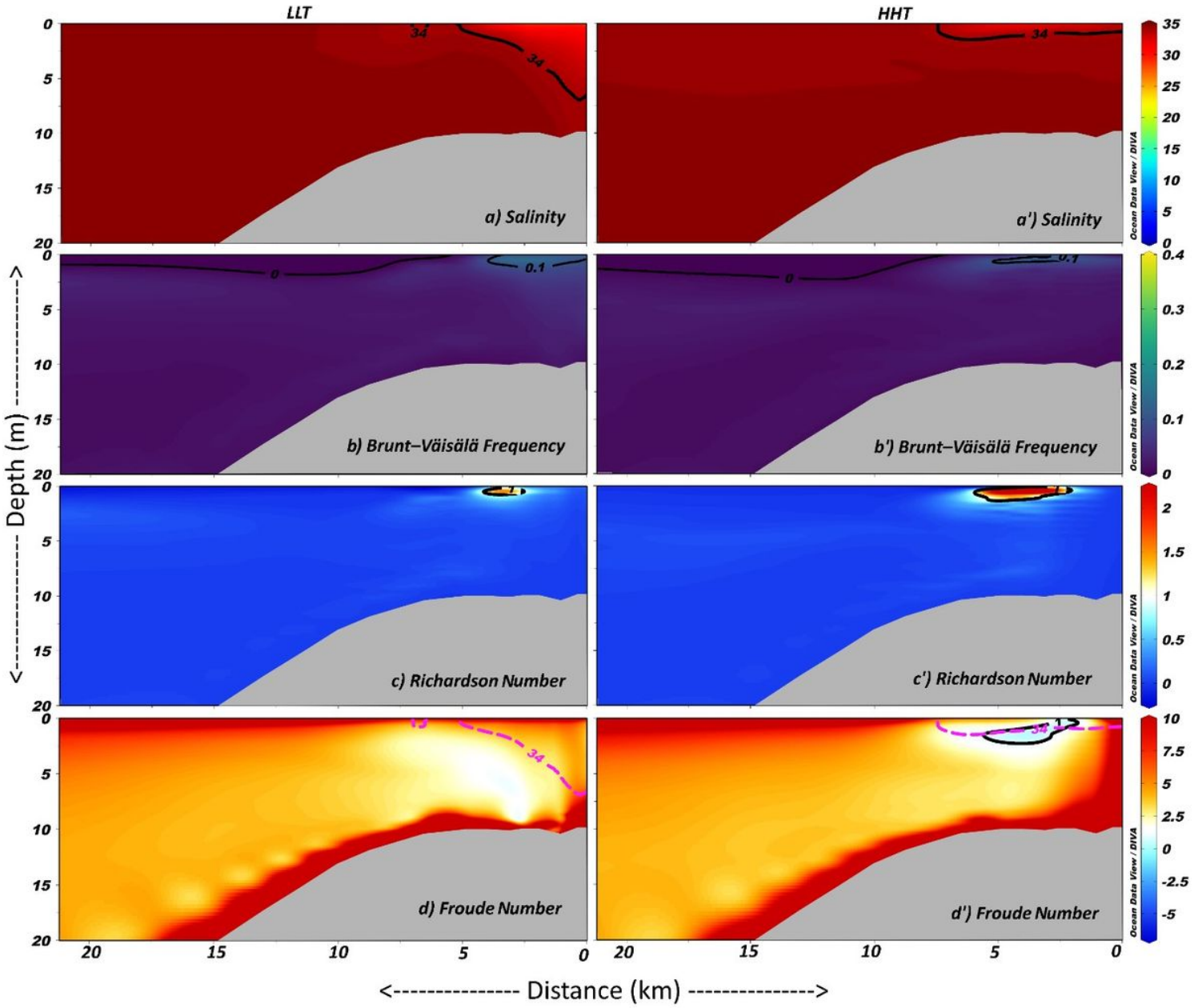

Figure 6

The horizontal and vertical extension of front, and variations in BVF, Rd, and F in the SIM during LLT and HHT.

Supplementary Files

This is a list of supplementary files associated with this preprint. Click to download.

- Supplementaryfigures02032021.docx